Theory of low energy excitations in resonant inelastic x-ray scattering for rare-earth systems: Yb compounds as typical examples

A. Kotani*

Photon Factory, Institute of Materials Structure Science, High Energy Accelerator Research Organization, 1-1 Oho, Tsukuba, Ibaraki 305-0801, Japan

(Received 22 December 2010; revised manuscript received 3 March 2011; published 25 April 2011)

Theoretical predictions are given for low energy excitations, such as crystal field excitations and Kondo resonance excitations, to be detected by high-resolution measurements of resonant inelastic x-ray scattering (RIXS) of rare-earth materials with Yb compounds as typical examples. Crystal field excitations in the Yb 3*d* RIXS of a Yb^{3+} ion in the cubic crystal field are formulated, and the calculation of RIXS spectra for YbN is done. Kondo resonance excitations revealed in the Yb 3*d* RIXS spectra are calculated for mixed-valence Yb compounds, $Yb_{1-x}Lu_xAl_3$, in the leading term approximation of the $1/N_f$ expansion method with a single impurity Anderson model. It is emphasized that the high-resolution RIXS with polarization dependence is a powerful tool to study the crystal field levels together with their symmetry and also the Kondo bound state in rare-earth compounds. Some in-depth discussions are given on the polarization effects of RIXS, including 4*d* and 2*p* RIXS spectra, the coherence effect of the Kondo bound states, and the importance of the high-resolution RIXS spectra for condensed matter physics under extreme conditions.

DOI: 10.1103/PhysRevB.83.165126 PACS number(s): 78.70.Ck, 71.28.+d, 71.27.+a, 71.70.Ch

I. INTRODUCTION

Resonant inelastic x-ray scattering (RIXS) is a powerful tool for the study of electronic states and collective excitations in highly correlated systems such as rare-earth (RE) compounds and transition metal (TM) compounds (see, for instance, Refs. 1–3). In RIXS, a core electron is excited by an incident x-ray photon whose energy is close to the corresponding absorption threshold, and then the excited state decays by emitting an x-ray photon. Therefore, the energy transfer and the momentum transfer, respectively, of the RIXS spectra correspond to the energy and momentum of the elementary excitations occurring in the material system. RIXS provides us with bulk-sensitive and site-selective information, and the technique can be applied equally to metals and insulators. Furthermore, RIXS can be performed in the applied electric or magnetic fields, as well as under high pressure, since it is a photon-in–photon-out process.

The recent progress in high-resolution RIXS measurements has enabled the detection of low-energy inelastic scattering peaks that can be separated from an elastic scattering peak. Typical examples are magnon excitations and orbital excitations in TM 2*p* RIXS of TM compounds.[4–7] However, most high-resolution RIXS experiments done so far have been limited to TM compounds. A considerable number of RIXS experiments were also performed at the RE 3*d* edge in RE compounds,[8–10] but they were not high-resolution measurements to reveal the low energy elementary excitations. The purpose of the present paper is to emphasize the importance of high-resolution RIXS for RE compounds from a theoretical viewpoint by calculating RIXS spectra for Yb compounds.

We give theoretical predictions for crystal field excitations and Kondo resonance excitations in the Yb 3*d* RIXS of Yb compounds. The energy of crystal field excitations in RE systems is one or two orders of magnitude smaller than that in TM systems, but it has been almost possible to observe them using high-resolution RIXS techniques. As an example, we calculate the crystal field excitations in the Yb 3*d* RIXS spectra for YbN, where the cubic crystal field acts on the Yb 4*f* electrons. It is shown that precise information on the crystal field energy levels and their symmetries can be obtained by high-resolution RIXS experiments with polarization dependence.

Another interesting RIXS experiment is the detection of the Kondo resonance excitation in mixed-valence (or intermediate valence) RE compounds. We give a formulation to calculate the Yb 3*d* RIXS of mixed-valence Yb compounds in the leading term approximation of the $1/N_f$ expansion method with the single impurity Anderson model (SIAM).[11,12] The ground state of mixed-valence Yb compounds is a singlet bound state called the Kondo bound state. The binding energy k_BT_K is called the Kondo binding energy and the temperature T_K the Kondo temperature. The electronic excitations from the Kondo bound state to low-lying continuous energy states are expected to be detected by high-resolution RIXS. We call this excitation " Kondo resonance excitation." As an example, we calculate the Yb 3*d* RIXS spectra for $Yb_{1-x}Lu_xAl_3$, which is an interesting alloy system whose Kondo temperature changes dramatically with x: $T_K = 670$, 1071, 1642, and 2386 K for $x = 0$, 0.1, 0.3, and 0.5, respectively.[13] It is shown that Kondo resonance excitation is reflected strongly in high-resolution RIXS spectra with a clear polarization dependence. Although the intersite coherence effect of the Kondo bound states cannot be treated by SIAM, it would be reasonable to calculate the RIXS spectra with SIAM as a starting model, because a variety of core-level spectroscopies for mixed-valence RE compounds (even with a periodic arrangement of RE atoms) are well explained by SIAM (see, for instance, a review article by de Groot and Kotani[3]). Some discussions will also be given to address the coherence effect.

The organization of the present paper is as follows: In Sec. II, we describe the Yb 4*f* electron states in the cubic crystal field, and we calculate the Yb 3*d* RIXS spectra corresponding to crystal field excitations in YbN. In Sec. III, the calculation of the Kondo bound state and excited states is done for

mixed-valence Yb compounds in the lowest order approximation of the $1/N_f$ expansion method with SIAM. The Yb $3d$ RIXS spectra are calculated to reveal the Kondo resonance excitation of $Yb_{1-x}Lu_xAl_3$. Section IV is devoted to discussions.

II. CRYSTAL FIELD EXCITATION

We consider a trivalent Yb ion in the cubic crystal field. The $4f$ electrons are in the $4f^{13}$ configuration, and by the spin-orbit interaction the $4f$ level is split into $J = 7/2$ and $5/2$ levels, where J is the total angular momentum of the $4f^{13}$ configuration. Since the energy of the $J = 7/2$ level is lower than that of the $J = 5/2$ level by about 1.5 eV, we take into account only the $J = 7/2$ states, as we are interested in the low energy RIXS excitation of energy transfer well below 1.0 eV.

The Hamiltonian of the cubic crystal field acting on the $4f$ electrons with $J = 7/2$ ($J_z = -7/2 \sim 7/2$) is written as[14–17]

$$H^{(c)} = B_4\left(O_4^0 + 5O_4^4\right) + B_6\left(O_6^0 - 21O_6^4\right), \tag{1}$$

where

$$O_4^0 = 35J_z^4 - [30j(j+1) - 25]J_z^2 - 6J(J+1) + 3j^2(J+1)^2, \tag{2}$$

$$O_4^4 = \tfrac{1}{2}(J_+^4 + J_-^4), \tag{3}$$

$$O_6^0 = 231J_z^6 - 105[3J(J+1) - 7]j_z^4 + [105J^2(J+1)^2 - 525J(J+1) + 294]J_z^2 - 5J^3(J+1)^3 + 40J^2(J+1)^2 - 60j(J+1), \tag{4}$$

$$O_6^4 = \tfrac{1}{4}\left[11J_z^2 - J(J+1) - 38\right]\left(J_+^4 + J_-^4\right) + \tfrac{1}{4}(J_+^4 + J_-^4)\left[11J_z^2 - J(J+1) - 38\right]. \tag{5}$$

The Hamiltonian is easily diagonalized, and the $J = 7/2$ level with eightfold degeneracy splits into three levels that are denoted by Γ_6 (twofold degeneracy), Γ_7 (twofold degeneracy), and Γ_8 (threefold degeneracy). The energy eigenvalues are given by Lea, Leask, and Wolf[16] as shown in Fig. 1, where W and x are related with B_4 and B_6 by the following equations:

$$60B_4 = Wx, \tag{6}$$

$$1260B_6 = W(1 - |x|). \tag{7}$$

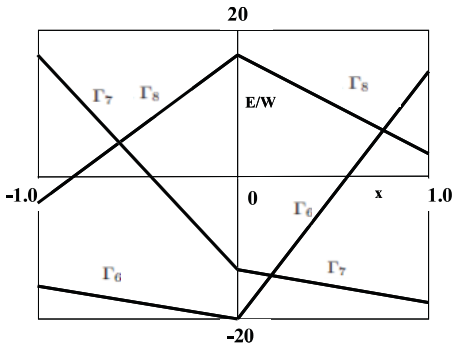

FIG. 1. Crystal field levels of $4f$ states of a Yb^{3+} ion.

The abscissa and ordinate of this figure are taken as x and the energy eigenvalue normalized by W, respectively. The energy eigenfunctions are given by

$$|\Gamma_6(\alpha = 1,2)\rangle = \sqrt{5/12}|\pm 7/2\rangle + \sqrt{7/12}|\mp 1/2\rangle, \tag{8}$$

$$|\Gamma_7(\alpha = 1,2)\rangle = \sqrt{3}/2|\pm 5/2\rangle - 1/2|\mp 3/2\rangle, \tag{9}$$

$$|\Gamma_8(\alpha = 1,2)\rangle = \sqrt{7/12}|\pm 7/2\rangle - \sqrt{5/12}|\mp 1/2\rangle, \tag{10}$$

$$|\Gamma_8(\alpha = 3,4)\rangle = 1/2|\pm 5/2\rangle + \sqrt{3}/2|\mp 13/2\rangle, \tag{11}$$

where α is the index representing the degeneracy of the irreversible representation; for instance, the states of $\alpha = 1$ and 2 in Eq. (8) are given by the wave functions with upper and lower signs, respectively, on the right-hand side.

Now we consider an RIXS process where an Yb $3d$ electron is excited to the Yb $4f$ state by the incident photon and an Yb $4f$ electron is deexcited to the Yb $3d$ state by emitting a photon. The RIXS spectrum is expressed as the coherent second-order optical formula in the following form:

$$F_{q_2,q_1}(\Omega,\omega) = \sum_{j,g}\left|\sum_i \frac{\langle j|C_{q_2}^{(1)}|i\rangle\langle i|C_{q_1}^{(1)}|g\rangle}{E_g + \Omega - E_i + i\Gamma}\right|^2 \times G(\Omega - \omega - E_j + E_g), \tag{12}$$

where Ω and ω, respectively, are the energies of the incident and emitted photons, q_1 and q_2 are their polarizations, and $C_q^{(1)}$ is the spherical tensor operator corresponding to the electric dipole transition, so that the polarizations $q = 1$, 0, and -1 represent $+$helicity, linear, and $-$helicity polarizations, respectively. The states $|g\rangle$, $|i\rangle$, and $|j\rangle$ are initial, intermediate, and final states of the electronic system, E_g, E_i, and E_j are their energies, Γ is the lifetime broadening of the $3d$ core hole, and $G(x)$ is the Gaussian function representing the experimental resolution:

$$G(x) = \sqrt{\frac{4\log 2}{\pi R^2}}\exp\left(-\frac{4(\log 2)x^2}{R^2}\right), \tag{13}$$

where R is the resolution given by the full width at half maximum (FWHM). Since the three crystal field levels are all degenerate, the summation over g (the degenerate ground states) is necessary in Eq. (12).

As a typical example in the calculation of RIXS spectra, we consider YbN. According to neutron inelastic scattering measurements,[18] the ground state of the Yb $4f$ states of YbN is Γ_6, and the energy difference between Γ_8 and Γ_6 and that between Γ_7 and Γ_6 are 33 and 81 meV, respectively, as shown in Fig. 2. The values of B_4 and B_6 are -0.042 and 0.000 06 meV, respectively. Following the $3d$ to $4f$ excitation caused by the

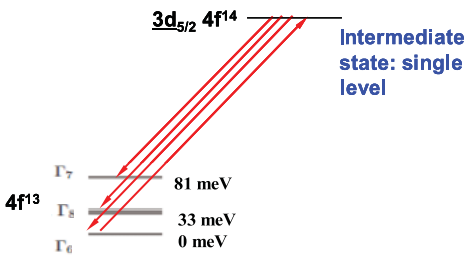

FIG. 2. (Color online) Schematic RIXS transition processes for crystal field excitations of YbN.

TABLE I. Values of $\langle 3d; j_z|C_1^{(1)}|4f; \Gamma_i(\alpha)\rangle$.

j_z	$\Gamma_6(1)$	$\Gamma_6(2)$	$\Gamma_8(1)$	$\Gamma_8(2)$	$\Gamma_8(3)$	$\Gamma_8(4)$	$\Gamma_7(1)$	$\Gamma_7(2)$
5/2	0	$\sqrt{5/12}$	0	0	0	$\sqrt{7/12}$	0	0
3/2	0	0	0	$\sqrt{5/28}$	0	0	$\sqrt{15/28}$	0
1/2	0	0	0	0	$\sqrt{5/14}$	0	0	$-\sqrt{5/42}$
−1/2	$\sqrt{1/6}$	0	$-\sqrt{5/42}$	0	0	0	0	0
−2/3	0	$\sqrt{1/12}$	0	0	0	$-\sqrt{5/84}$	0	0
−5/2	0	0	0	$\sqrt{1/28}$	0	0	$-\sqrt{1/84}$	0

incident photon, we have a $3d_{5/2}4f^{14}$ configuration, which is a single level because the $\overline{4f}$ shell is filled and a $3d$ core hole is only allowed for the $J_{3d} = 5/2$ (the transition from $J_{3d} = 3/2$ to $J_{4f} = 7/2$ is dipole-forbidden). Then one of the $4f$ electrons in the filled $4f$ shell makes a transition to the $3d$ state. If the final state is the Γ_6 states, we have an elastic scattering line, and if it is the Γ_8 or Γ_7 states, we have inelastic scattering spectra.

The states $|g\rangle$, $|i\rangle$, and $|j\rangle$ in Eq. (12) are many-body electronic states, but the dipole matrix elements between them can be replaced by single-electron transition matrix elements, and after some manipulation $F_{q_2,q_1}(\Omega,\omega)$ is rewritten as

$$F_{q_2,q_1}(\Omega,\omega) = \sum_{i,\alpha,\alpha'} \Bigg| \sum_{j_z} \langle 3d; j_z \big| C_{q_2}^{(1)} | 4f; \Gamma_i(\alpha)\rangle \langle 4f; \Gamma_6(\alpha') \times |C_{q_1}^{(1)}|3d; j_z\rangle \Big|^2 G[\Omega - \omega - E(\Gamma_i) + E(\Gamma_6)]/\Gamma^2, \quad (14)$$

where the incident photon energy is tuned to the resonance energy (the energy difference between the single intermediate state and the ground state). The matrix element $\langle 3d; j_z|C_{q_2}^{(1)}|4f; \Gamma_i(\alpha)\rangle$ is that of the single electron dipole transition from the $4f$ state with $\Gamma_i(\alpha)$ to the $3d$ state with j_z, and is expressed as

$$\langle 3d; j_z|C_q^{(1)}|4f; \Gamma_i(\alpha)\rangle = \sum_{j_z'} \langle 5/2\ j_z\ 1\ q|7/2\ j_z'\rangle \langle 7/2; j_z'|4f; \Gamma_i(\alpha)\rangle, \quad (15)$$

where $\langle 5/2\ j_z\ 1\ q|7/2\ j_z'\rangle$ are the Clebsh-Gordan coefficients, and $\langle 7/2; j_z'|4f; \Gamma_i(\alpha)\rangle$ are the same as the coefficients on the right-hand sides of Eqs. (8)–(11). We list the values of $\langle 3d; j_z|C_q^{(1)}|4f; \Gamma_i(\alpha)\rangle$ for $q = 1, 0$, and -1 in Tables I, II, and III, respectively.

Some results of the calculated spectra are shown in Fig. 3, where the polarizations (q_2,q_1) are taken as (1, 1) and (1, 0), and the resolution R is changed as a parameter. The value of Γ is taken to be 0.7 eV. It is found that one elastic and two inelastic scattering peaks are clearly seen if the resolution is high enough. An important point is that the RIXS spectra due to the crystal field excitations exhibit a strong polarization dependence, which reflects the symmetry of the wave functions of the crystal field levels. Therefore, by analyzing the polarization dependence of the RIXS signal, we can obtain precise information on the energies and symmetries of the crystal field levels.

In realistic measurements of RIXS spectra, the linear polarization is more frequently used than the circular polarization, and the polarization of the emitted photon is not detected. The polarization geometry that is conventionally used is shown in Fig. 4. The scattering angle is 90°, and in Fig. 4(a) the incident polarization is perpendicular to the scattering plane, whereas in Fig. 4(b) the incident polarization is in the scattering plane. The former and latter geometries are referred to as the polarized and depolarized geometries, respectively. As shown by Nakazawa *et al.*,[19] the RIXS spectra in the polarized geometry $F_{\rm pol}$ and the depolarized geometry $F_{\rm depol}$ are given, in terms of F_{q_1,q_2}, by

$$F_{\rm pol} = F_{0,0} + (F_{1,0} + F_{-1,0})/2, \quad (16)$$

$$F_{\rm depol} = F_{1,0} + F_{-1,0}. \quad (17)$$

To calculate $F_{\rm pol}$ and $F_{\rm depol}$, we calculate $F_{1,0}$, $F_{-1,0}$, and $F_{0,0}$ in addition to $F_{1,1}$ and $F_{-1,1}$, and the results are shown in Fig. 5. The resolution is taken to be $R = 20$ meV. Because of the cubic symmetry, the spectra $F_{1,0}$ and $F_{-1,0}$ are the same, and of the four curves shown in Fig. 5, the number of independent spectra is two.

The results of $F_{\rm pol}$ and $F_{\rm depol}$ are shown in Fig. 6. The polarization dependence between $F_{\rm pol}$ and $F_{\rm depol}$ is seen to be very large, so that the measurements of both spectra will

TABLE II. Values of $\langle 3d; j_z|C_0^{(1)}|4f; \Gamma_i(\alpha)\rangle$.

j_z	$\Gamma_6(1)$	$\Gamma_6(2)$	$\Gamma_8(1)$	$\Gamma_8(2)$	$\Gamma_8(3)$	$\Gamma_8(4)$	$\Gamma_7(1)$	$\Gamma_7(2)$
5/2	0	0	0	$\sqrt{1/14}$	0	0	$\sqrt{3/14}$	0
3/2	0	0	0	0	$\sqrt{5/14}$	0	0	$-\sqrt{5/42}$
1/2	$\sqrt{1/3}$	0	$-\sqrt{5/21}$	0	0	0	0	0
−1/2	0	$\sqrt{1/3}$	0	0	0	$-\sqrt{5/21}$	0	0
−2/3	0	0	0	$\sqrt{5/14}$	0	0	$-\sqrt{5/42}$	0
−5/2	0	0	0	0	$\sqrt{1/14}$	0	0	$\sqrt{3/14}$

TABLE III. Values of $\langle 3d; j_z|C^{(1)}_{-1}|4f; \Gamma_i(\alpha)\rangle$.

j_z	$\Gamma_6(1)$	$\Gamma_6(2)$	$\Gamma_8(1)$	$\Gamma_8(2)$	$\Gamma_8(3)$	$\Gamma_8(4)$	$\Gamma_7(1)$	$\Gamma_7(2)$
5/2	0	0	0	0	$\sqrt{1/28}$	0	0	$-\sqrt{1/84}$
3/2	$\sqrt{1/12}$	0	$-\sqrt{5/84}$	0	0	0	0	0
1/2	0	$\sqrt{1/6}$	0	0	0	$-\sqrt{5/42}$	0	0
−1/2	0	0	0	$\sqrt{5/14}$	0	0	$-\sqrt{5/42}$	0
−2/3	0	0	0	0	$\sqrt{5/28}$	0	0	$\sqrt{15/28}$
−5/2	$\sqrt{5/12}$	0	$\sqrt{7/12}$	0	0	0	0	0

yield important information on the symmetry of the crystal field states. If the experimental resolution becomes sufficiently high, RIXS will be the most powerful tool for the study of crystal field states in RE systems. As will be discussed in Sec. IV, we can calculate, by using Tables I, II, and III, the RIXS spectra of Yb^{3+} states in the cubic crystal field for any values of B_4 and B_6, so that we can easily analyze experimental data of RIXS and estimate the values of B_4 and B_6.

III. KONDO RESONANCE EXCITATION

We consider a mixed-valence Yb compound and calculate the electronic states with SIAM.[11,12] The Hamiltonian of the system is given by

$$H = \sum_{\nu} \epsilon_{f,\nu} f^{\dagger}_{\nu} f_{\nu} + \sum_{\mu} \epsilon_{d,\mu} d^{\dagger}_{\mu} d_{\mu} + \sum_{k,\nu} \epsilon_k c^{\dagger}_{k,\nu} c_{k,\nu} + \sum_{k,\nu} V_{k,\nu} (c^{\dagger}_{k,\nu} f_{\nu} + f^{\dagger}_{\nu} c_{k,\nu}) + U_{ff} \sum_{\nu>\nu'} f^{\dagger}_{\nu} f_{\nu} f^{\dagger}_{\nu'} f_{\nu'} - U_{fc} \sum_{\nu,\mu} f^{\dagger}_{f,\nu} f_{f,\nu} (1 - d^{\dagger}_{p,\mu} d_{p,\mu}), \quad (18)$$

where the first, second, and third terms represent, respectively, the single electron energies of the Ce $4f$ states, the Ce $3d$ core states, and the conduction band, the fourth term is the hybridization between the Ce $4f$ and the conduction-band states, the fifth term is the Coulomb interaction between Ce $4f$ electrons, and the last term is the attractive $3d$ core-hole potential acting on the $4f$ state. The Ce $4f$ and $3d$ states are represented in the JJ coupling scheme, and indices ν and μ denote a set of quantum numbers (j, j_z) and (j', j'_z) of the $4f$ and $3d$ states, respectively, where we take $j = 7/2$ and then the electric dipole transition is allowed only for $j' = 5/2$, as mentioned before.

The density of states of the conduction band is assumed to be of rectangular shape with width W. The conduction band is assumed to be half-filled after Ref. 20. The energy levels of the conduction band are treated as N discrete levels:

$$\epsilon_k = \frac{W}{2N}(2k - N - 1), \quad (19)$$

where $k = 1, 2, \ldots, N$, and the Fermi level ϵ_F is located at the center of the band. The hybridization matrix element $V_{k,\nu}$ is treated to be independent of k and ν, and we set $V_{k,\nu} = V/\sqrt{N}$ with a constant V. In the following, we assume $U_{ff} = \infty$, and make our calculation within the leading term approximation in the $1/N_f$ expansion method,[11] where N_f is the degeneracy of the $4f$ states ($N_f = 2j + 1 = 8$).

The ground state $|g\rangle$ of the Hamiltonian is written as

$$|g\rangle = a^{(g)}_0 \left(|0\rangle + \frac{1}{N_f} \sum_{k,j_z} b^{(g)}(k) c^{\dagger}_{k,j_z} f_{j_z} |0\rangle \right), \quad (20)$$

where $|0\rangle$ is the state in which the $4f$ shell is filled and all other electronic states below ϵ_F are also filled. The expression of the ground state is essentially the same as that given by Eq. (11) of Ref. 20, although the electron picture is used in the present paper whereas the hole picture is used in Ref. 20. The ground state is the singlet bound state denoted by the Kondo bound state (unless V is zero), and the Kondo binding energy $k_B T_K$ is easily obtained in the limit of $N \to \infty$:[20] The value of $k_B T_K$ is calculated by solving the following equation:

$$k_B T_K - \epsilon_f + \frac{N_f V^2}{W} \left[\log(k_B T_K) - \log\left(k_B T_K + \frac{W}{2} \right) \right] = 0, \quad (21)$$

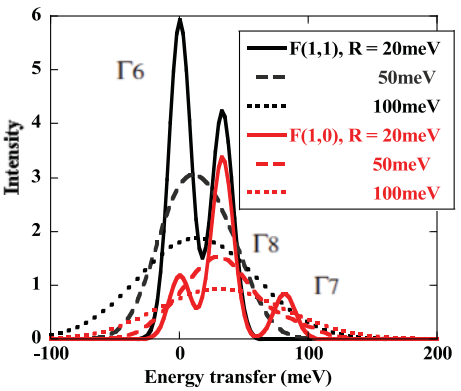

FIG. 3. (Color online) Calculated RIXS spectra by crystal field excitations of YbN for the polarization components $(q_1, q_2) = (1, 1)$ and $(1, 0)$. The resolution R is taken to be 20, 50, and 100 meV.

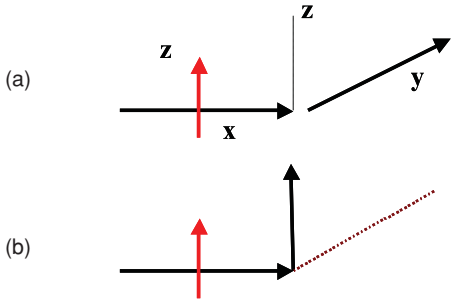

FIG. 4. (Color online) (a) Polarized geometry and (b) depolarized geometry.

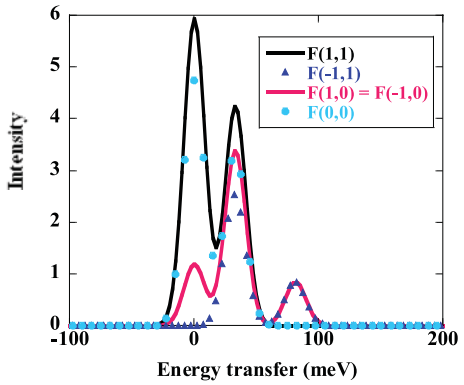

FIG. 5. (Color online) Calculated RIXS spectra by crystal field excitations of YbN for various polarization components (q_1,q_2). The resolution R is taken to be 20 meV.

and if we obtain k_BT_K, the $4f$ hole number n_f (the $4f$ electron number is $14-n_f$) is given by

$$n_f = \frac{N_f V^2}{2k_BT_K\left(k_BT_K + \frac{W}{2}\right) + N_f V^2}. \tag{22}$$

See Ref. 20 for the derivation of Eqs. (21) and (22). The assumption of the half-filled conduction band does not affect seriously the following results of the calculated RIXS spectra, as will be mentioned.

Now we consider the RIXS spectra corresponding to Yb $3d$-$4f$ excitation and $4f$-$3d$ de-excitation. The optical transition process is shown schematically in Fig. 7. The ground state is the Kondo singlet bound state given by Eq. (20), which is a linear combination of the $4f^{14}$ and $4f^{13}c_k$ configurations, where c_k is a conduction electron above ϵ_F. In the intermediate state $|i\rangle$, a $3d_{5/2}$ electron is excited to the $4f$ state, so that we have the $\underline{3d_{5/2}}4f^{14}c_k$ configuration expressed by

$$|i\rangle = c^\dagger_{kj_z} d_{j'_z}|0\rangle. \tag{23}$$

For the elastic scattering, the final state is $|g\rangle$, and for the inelastic scattering the final states $|j\rangle$ are given by

$$|j\rangle = a_0^{(j)}\left(|0\rangle + \frac{1}{N_f}\sum_{k,j_z} b^{(j)}(k)c^\dagger_{k,j_z} f_{j_z}|0\rangle\right), \tag{24}$$

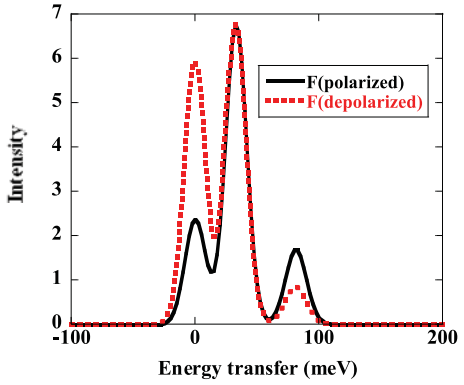

FIG. 6. (Color online) Calculated RIXS spectra by crystal field excitations of YbN for the polarized and depolarized geometries. The resolution R is taken to be 20 meV.

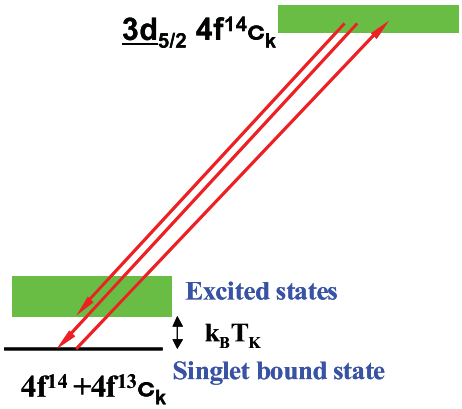

FIG. 7. (Color online) Schematic RIXS transition processes for the Kondo resonance excitation in a mixed-valence Yb compound.

which are orthogonal with $|g\rangle$. The states $|j\rangle$ form a continuous excitation band, the bottom of which is located by k_BT_K above the ground state (the Kondo bound state). In addition to $|j\rangle$, we have to take into account the other type of final states, $|j^*\rangle$, given by

$$|j^*\rangle = c^\dagger_{k,j_z} f_{j^*_z}|0\rangle, \tag{25}$$

where $j_z \neq j^*_z$. The states $|j^*\rangle$ are in the $4f^{13}c_k$ configurations, but they do not couple with the $4f^{14}$ configuration by the hybridization V, so that we call them "nonbonding states."

Within our SIAM, all electronic states are determined if we fix the parameter values V and ϵ_f. Furthermore, the values of V and ϵ_f are obtained from Eqs. (21) and (22) if we give the values of k_BT_K and n_f. To make explicit calculations of RIXS spectra, we consider the alloy system $Yb_{1-x}Lu_xAl_3$. Based on the experimental results obtained by x-ray absorption spectra (XAS) at the Yb L_3 edge and magnetic susceptibility, k_BT_K and n_f of $Yb_{1-x}Lu_xAl_3$ change with x as shown in Figs. 8(a) and 8(b), respectively.[13] Then, the x dependences of V and ϵ_f are obtained from Eqs. (21) and (22) as shown in Figs. 9(a) and 9(b), respectively, where we assumed $W = 2.0$ eV. Using these values of V and ϵ_f, we diagonalize the Hamiltonian H with $N = 200$, and calculate the spectra of $3d$ XAS and $3d$ RIXS with $\Gamma = 0.7$ eV [using Eq. (12) for RIXS]. Since the present ground state has no degeneracy, the summation over g in Eq. (12) is removed.

Here it should be mentioned that the values of V and ϵ_f are strongly model-dependent; for the same values of k_BT_K and n_f, the values of V and ϵ_f should be different if we use a different value of W and assume a different filling of conduction electrons from the half-filling. However, the calculated RIXS spectra are almost the same for the different values of V and ϵ_f if the values of k_BT_K and n_f are kept unchanged. The situation is very similar to what we showed in Ref. 20, i.e., if the values of k_BT_K and n_f are kept unchanged, the calculated x-ray magnetic circular dichroism (XMCD) spectra are almost the same for different values of the conduction-band width (and thus the different values of V and ϵ_f). In this sense, k_BT_K and n_f are more fundamental quantities than V and ϵ_f in the calculation of RIXS spectra. Bauer *et al.*[13] also reported the values of V and ϵ_f of $Yb_{1-x}Lu_xAl_3$, but their values are somewhat different from our values because their model is different from ours.

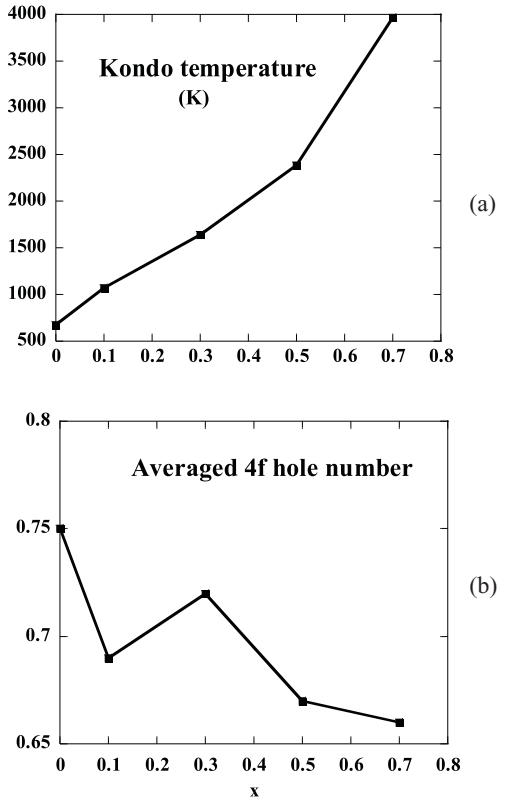

FIG. 8. Experimental results[13] of (a) the Kondo temperature and (b) the averaged $4f$ hole number of $Yb_{1-x}Lu_xAl_3$ as a function of x.

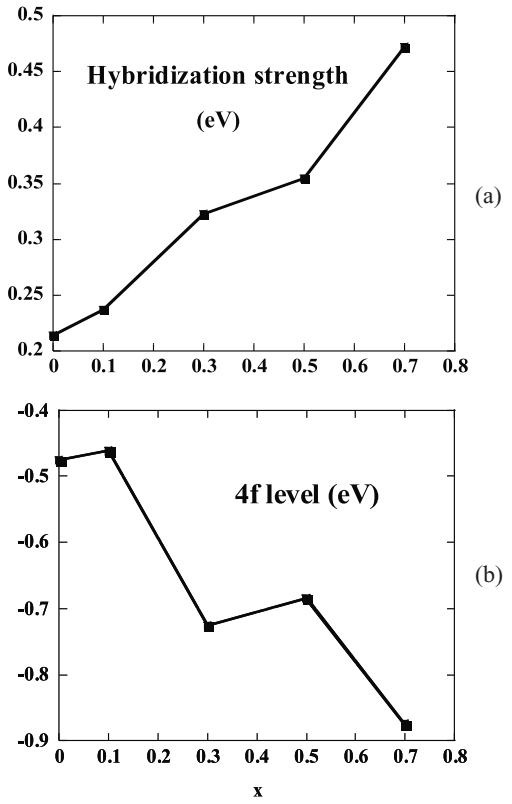

FIG. 9. (a) The hybridization strength and (b) the $4f$ level measured from the Fermi level in our model of $Yb_{1-x}Lu_xAl_3$ as a function of x.

The calculated Yb $3d$ XAS and Yb $3d$ RIXS (F_{q_2,q_1}) spectra are shown in Figs. 10 and 11, respectively. The XAS spectrum corresponds to transitions from the ground state to the intermediate states of RIXS by changing the incident photon energy. Now the intermediate state is not a single level; the peak position of XAS shifts slightly from the origin (which corresponds to the transition to the lowest edge of the intermediate states). For RIXS spectra in Fig. 11, the incident photon energy is fixed at the origin of Fig. 10, and the polarization geometry (q_2,q_1) is taken to be (1,1) with the resolution $R = 45$ meV.

If the resolution is sufficiently high, the Kondo resonance is clearly seen as an RIXS structure, so that the RIXS measurements can be a powerful tool to observe directly the Kondo temperature. The calculated RIXS spectra for polarized and depolarized geometries are shown in Figs. 12(a) and 12(b), respectively, with the resolution $R = 45$ and 100 meV and with $x = 0$ and 0.5, where $F_{\rm pol}$ and $F_{\rm depol}$ are obtained by Eqs. (14) and (15), respectively. A significant polarization dependence is recognized.

IV. DISCUSSIONS

We showed by theoretical calculations that high-resolution RIXS can be used as a powerful means to study the crystal field states and the Kondo bound state of Yb compounds. So far, crystal field excitation has mainly been measured by inelastic neutron scattering experiments[18,21,22] and Kondo resonance excitation by optical conductivity[23–26] and inelastic neutron scattering measurements,[27] but virtually no RIXS measurement has been reported yet. Very recently, Hancock[28] succeeded in measuring Kondo resonance excitation (or hybridization gap excitation) of $YbInCu_4$ by Yb $3d$ RIXS, but the resolution (200 meV) is not sufficiently high for this purpose. RIXS measurements with a higher resolution are highly desired for the observation of crystal field and Kondo excitations.

As shown in this paper, strong polarization dependence is a characteristic feature of RIXS spectra. Comparing Figs. 5 and 12, we recognize a considerable difference in the polarization dependences of crystal field excitation and Kondo resonance

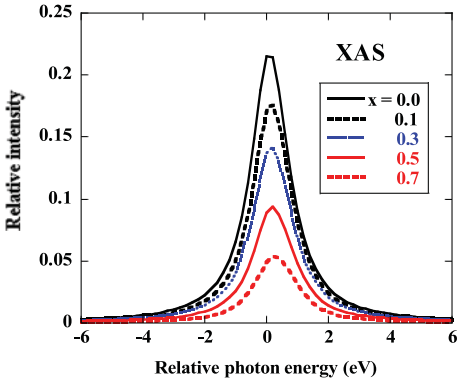

FIG. 10. (Color online) Calculated Yb $3d$ XAS spectra for $Yb_{1-x}Lu_xAl_3$ for various values of x. The absolute energy of the Yb $3d_{5/2}$ resonant excitation is about 1518 eV.

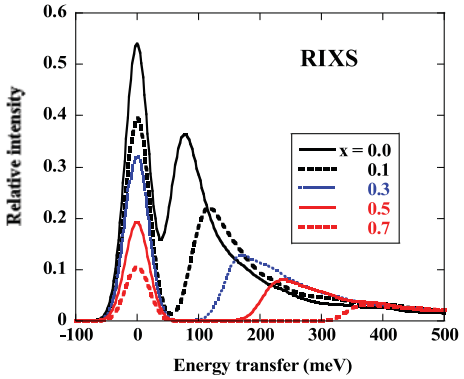

FIG. 11. (Color online) Calculated Yb $3d$ RIXS spectra for $Yb_{1-x}Lu_xAl_3$ for various values of x. The polarizations (q_1,q_2) and the resolution R are taken to be (1, 1) and 45 meV, respectively.

excitation. For crystal field excitation, the intensity of the elastic scattering is larger for depolarized geometry than for polarized geometry, while for Kondo resonance excitation the elastic-scattering intensity is finite for polarized geometry but it vanishes for depolarized geometry. It was first explained by Matsubara *et al.*[29] that the elastic scattering intensity should vanish in the depolarized geometry for the Ti $2p$ RIXS of TiO_2 because the ground state is a nondegenerate singlet state. Nakazawa *et al.*[19] also showed the same effect for the Ce $3d$ RIXS of CeO_2. The same explanation can be applied to the present case, because the Kondo ground state is a nondegenerate singlet bound state. The vanishing elastic-scattering intensity of TiO_2 in the depolarized geometry was also confirmed experimentally by Harada *et al.*[30] However, by considering that TiO_2 and CeO_2 are insulators but $Yb_{1-x}Lu_xAl_3$ is metallic, the situation might be somewhat different. In our calculation, we took into account only the f symmetric component of conduction electrons, but actually the components of the other symmetries (s, p, d, and so on) coexist as metallic conduction electrons. Therefore, for $Yb_{1-x}Lu_xAl_3$, quasielastic scatterings very close to the elastic line might be caused by these conduction electrons even in the depolarized geometry. On the other hand, for the crystal field excitation treated here, the ground state has twofold degeneracy, and this is why the elastic scattering intensity does not vanish in the depolarized geometry. It should also be mentioned that we disregarded Thomson scattering, which might be superposed on resonant scattering (especially for elastic scattering) with a different polarization dependence from that of resonance scattering.

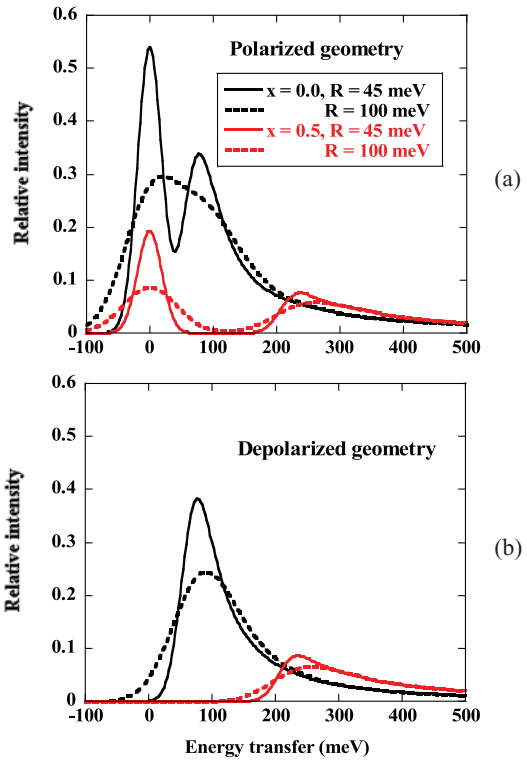

FIG. 12. (Color online) Calculated Yb $3d$ RIXS spectra of $Yb_{1-x}Lu_xAl_3$ for $x = 0$ and 0.5 in the (a) polarized and (b) depolarized geometries. The resolution R is taken to be 45 and 100 meV.

For the RIXS spectra of Yb^{3+} states in the cubic crystal field, we can easily calculate the spectra for any values of B_4 and B_6 (or W and x) by using Eq. (14), Fig. 1, and Tables I, II, and III. If the ground state is not Γ_6 but Γ_8 or Γ_7, Γ_6 in Eq. (14) should be replaced by Γ_8 or Γ_7, but the remaining calculations can be made in quite the same way as given in this paper.

For the RIXS spectra of mixed-valence Yb compounds, we confined ourselves to the Yb $3d$ edge, but the present results can be applied to the Yb $4d$ edge by a slight modification. The modification is caused only by the lifetime broadening of the core hole; the value of Γ is about 0.7 eV for Yb $3d$ RIXS but it is about 1.5 eV for Yb $4d$ RIXS. Knowing that the energy resolution of Yb $4d$ RIXS should be higher than that of Yb $3d$ RIXS, measurements of Kondo resonance excitation at the $4d$ edge should be of prime interest. Preliminary measurements of the Yb $4d$ RIXS spectra of $Yb_{1-x}Lu_xAl_3$ are now in progress to detect Kondo resonant excitations.[31] We note that, in the hard-x-ray range, Yb $2p$ RIXS may be another promising experiment. The obtained spectra are expected to be sensitive to Kondo resonant excitation but much less to crystal field excitation.

The present theory could be extended to Ce compounds. The ground state of the mixed-valence Ce $4f$ electrons is described in a similar way to that of the Yb $4f$ electrons by taking advantage of the electron-hole symmetry for the Ce and Yb $4f$ states. However, the calculation of the Ce $3d$ RIXS spectra is more complicated than it is for Yb, because the intermediate state is not a simple $4f^{14}$ configuration but rather the hybridized $4f^1$ and $4f^2$ configurations. Furthermore, the spin-orbit splitting of the Ce $4f$ state is about 200 meV, which is much smaller than that of the Yb $4f$ state (about 1.0 eV), so that the spin-orbit excitation peak may overlap in the same energy-transfer range as the Kondo excitations in the RIXS spectra. It is necessary to take into account both $J = 5/2$ and $7/2$ of the $4f$ states in the RIXS calculations of Ce compounds.

It has to be mentioned that in the present paper we confined ourselves to the SIAM calculations so that the intersite coherence effect of the Kondo bound states was neglected. In mixed-valence systems, the Kondo bound states are incoherent for the temperature range $T_K > T > T^*$, where T^* is called the coherence temperature, but below T^* they form a coherent quasiparticle band due to the effect of intersite coherence. To

take into account the coherence effect, it would be necessary to treat the periodic Anderson model instead of SIAM. According to the experimental results of Cornelius *et al.*[32] and Bauer *et al.*,[13] T^* of $YbAl_3$ is about 40 K, but the coherence effect is suppressed (so that $T^* \sim 0$) by only a small amount of Lu ($x > 0.05$) for $Yb_{1-x}Lu_xAl_3$. Therefore, the present theory would work better in the case of $x > 0.05$ than $x = 0$. According to optical conductivity measurements of $YbAl_3$ by Okamura *et al.*,[25] a midinfrared absorption peak was observed below T^* that was interpreted as an excitation across the hybridization gap due to the coherence effect (see also Refs. 23, 24, and 26 for other Yb compounds). It would be interesting to observe experimentally the temperature dependence of the RIXS spectra of $YbAl_3$ ($x = 0$) across T^* to see the coherence effect. Also, it would be interesting to compare the present theoretical RIXS spectra with experimental results for both $x = 0$ and $x > 0.05$ to investigate the coherence effect.

The momentum dependence of Kondo resonance excitation could be measured by Yb $2p$ RIXS, whereas the $3d$ and $4d$ RIXS detect only a fixed or zero momentum excitation. If the coherence effect is important, the momentum dependence of Kondo resonance excitation (or hybridization gap excitation) will be observed, but the momentum dependence of Kondo resonance excitation would be absent for $x > 0.05$ for $Yb_{1-x}Lu_xAl_3$. It is left to future investigations to calculate RIXS spectra with the periodic Anderson model.

Finally, we would like to emphasize that the high-resolution RIXS measurements in the hard-x-ray range are the best suited tool to address the Kondo problem under extreme conditions such as high magnetic fields and high pressures.[33] For instance, in $YbInCu_4$ the field-induced valence transition is observed, where the valence of Yb changes rapidly from 2.83 to 2.96 under around 30 T magnetic field at low temperatures.[35] The mechanism of this transition has not been well established, but it is expected, as a possibility, that the Kondo bound state (with or without the coherence effect) becomes unstable under an applied magnetic field of about 30 T. If high-resolution RIXS spectra of $YbInCu_4$ at the Yb $2p$ or $3d$ edge could be measured as a function of the magnetic-field strength, important information about the transition mechanism could be obtained directly by monitoring the Kondo resonance excitations under about 30 T magnetic field. Because photoemission spectroscopy cannot be used in high magnetic fields and high pressures, we anticipate that high-resolution RIXS will become an increasingly important means for condensed matter physics under extreme conditions.

ACKNOWLEDGMENTS

The main part of this paper was prepared during the author's temporary stay at ALS in Berkeley. The author would like to thank Z. Hussain and J.-H. Guo for their hospitality. The author also thanks J.-H. Guo, J. N. Hancock, I. Jarrige, and H. Yamaoka for useful discussions. This paper was partially supported by a Grant-in-Aid for Scientific Research C (No. 90029504) from the Japan Society for the Promotion of Science.

*Also at RIKEN Harima Institute, 1-1-1 Kouto, Sayo, Hyogo 679-5148, Japan; kotani@post.kek.jp

[1] A. Kotani and S. Shin, Rev. Mod. Phys. **73**, 203 (2001).
[2] A. Kotani, Eur. Phys. J. B **47**, 3 (2005).
[3] F. M. F. de Groot and A. Kotani, *Core Level Spectroscopy of Solids* (CRC, Boca Raton, FL, 2008).
[4] L. Braicovich, L. J. P. Ament, V. Bisogni, F. Forte, C. Aruta, G. Balestrino, N. B. Brookes, G. M. De Luca, P. G. Medaglia, F. Miletto Granozio, M. Radovic, M. Salluzzo, J. van den Brink, and G. Ghiringhelli, Phys. Rev. Lett. **102**, 167401 (2009).
[5] L. J. P. Ament, G. Ghiringhelli, M. M. Sala, L. Braicovich, and J. van den Brink, Phys. Rev. Lett. **103**, 117003 (2009).
[6] C. Ulrich, L. J. P. Ament, G. Ghiringhelli, L. Braicovich, M. M. Sala, N. Pezzotta, T. Schmitt, G. Khaliullin, J. van den Brink, H. Roth, T. Lorenz, and B. Keimer, Phys. Rev. Lett. **103**, 107205 (2009).
[7] J. Schlappa, T. Schmitt, F. Vernay, V. N. Strocov, V. Ilakovac, B. Thielemann, H. M. Ronnow, S. Vanishri, A. Piazzalunga, X. Wang, L. Braicovich, G. Ghiringhelli, C. Marin, J. Mesot, B. Delley, and L. Patthey, Phys. Rev. Lett. **103**, 047401 (2009).
[8] S. M. Butorin, D. C. Mancini, J. -H. Guo, N. Wassdahl, J. Nordgren, M. Nakazawa, S. Tanaka, T. Uozumi, A. Kotani, Y. Ma, K. E. Myano, B. A. Karlin, and D. K. Shuh, Phys. Rev. Lett. **77**, 574 (1996).
[9] S. M. Butorin, L.-C. Duda, J.-H. Guo, N. Wassdahl, J. Nordgren, M. Nakazawa, and A. Kotani, J. Phys. Condens. Matter **9**, 8155 (1997).
[10] M. Magnuson, S. M. Butorin, J.-H. Guo, A. Agui, J. Nordgren, H. Ogasawara, A. Kotani, T. Takahashi, and S. Kunii, Phys. Rev. B **63**, 75101 (2001).
[11] O. Gunnarsson and K. Schönhammer, Phys. Rev. B **28**, 4315 (1983).
[12] A. Kotani, T. Jo, and J. C. Parlebas, Adv. Phys. **37**, 37 (1988).
[13] E. D. Bauer, C. H. Booth, J. M. Lawrence, M. F. Hundley, J. L. Sarrao, J. D. Thompson, P. S. Riseborough, and T. Ebihara, Phys. Rev. B **69**, 125102 (2004).
[14] B. Breaney and K. W. H. Stevens, Rep. Prog. Phys. **16**, 108 (1952).
[15] J. M. Baker, B. Breaney, and W. Hayes, Proc. R. Soc. London, Ser. A **247**, 141 (1958).
[16] K. R. Lea, M. J. M. Leask, and W. P. Wolf, J. Phys. Chem. Solids **23**, 1381 (1962).
[17] M. T. Hutchings, in *Solid State Physics*, edited by F. Seitz and B. Turnbull (Academic, New York, 1965), Vol. 16, p. 227.
[18] A. Donni, A. Furrer, P. Fischer, F. Hulliger, and P. Wachter, Physica B **171**, 353 (1991).
[19] M. Nakazawa, H. Ogasawara, and A. Kotani, J. Phys. Soc. Jpn. **69**, 4071 (2000).
[20] A. Kotani, Eur. Phys. J. B **72**, 375 (2009).
[21] A. Severing, E. Gratz, B. D. Rainford, and K. Yoshimura, Physica B **163**, 409 (1990).
[22] A. Severing, A. P. Murani, J. D. Thompson, Z. Fisk, and C.-K. Loong, Phys. Rev. B **41**, 1739 (1990).
[23] J. N. Hancock, T. McKnew, Z. Schlesinger, J. L. Sarrao, and Z. Fisk, Phys. Rev. Lett. **92**, 186405 (2004).

[24] J. N. Hancock, T. McKnew, Z. Schlesinger, J. L. Sarrao, and Z. Fisk, Phys. Rev. B **73**, 125119 (2006).
[25] H. Okamura, T. Michizawa, T. Nanba, and T. Ebihara, Phys. Rev. B **75**, 041101 (2007).
[26] H. Okamura, T. Watanabe, M. Matsunami, T. Nishihara, N. Tsujii, T. Ebihara, H. Sugawara, H. Sato, Y. Onuki, Y. Ishikawa, T. Takabatake, and T. Nanba, J. Phys. Soc. Jpn. **76**, 023703 (2007).
[27] A. P. Murani, Phys. Rev. Lett. **54**, 1444 (1985).
[28] J. N. Hancock (unpublished).
[29] M. Matsubara, T. Uozumi, A. Kotani, Y. Harada, and S. Shin, J. Phys. Soc. Jpn. **69**, 1558 (2000).
[30] Y. Harada, T. Kinugasa, R. Eguchi, M. Matsubara, A. Kotani, M. Watanabe, A. Yagishita, and S. Shin, Phys. Rev. B **61**, 12854 (2000).
[31] J.-H. Guo (unpublished).
[32] A. L. Cornelius, J. M. Lawrence, T. Ebihara, P. S. Riseborough, C. H. Booth, M. F. Hundley, P. G. Pagliuso, J. L. Sarrao, J. D. Thompson, M. H. Jung, A. H. Lacerda, and G. H. Kwei, Phys. Rev. Lett. **88**, 117201 (2002).
[33] RIXS measurements in the soft-x-ray range under high pressures have not been reported so far, but XMCD measurements in high magnetic fields have very recently been performed successfully at RE 3*d* edges using a pulsed magnet up to 25 T.[34]
[34] M. Hayashi, Y. Narumi, H. Nojiri, T. Nakamura, T. Hirono, T. Kinoshita, K. Kodama, and K. Kindo, presented at the 37th International Conference on Vacuum Ultraviolet and X-ray Physics, Vancouver (2010); J. Electron Spectrosc. Relat. Phenom. (2011), doi:10.1016/j.elspec.2010.12.015.
[35] Y. H. Matsuda, T. Inami, K. Ohwada, Y. Murata, H. Nojiri, Y. Murakami, H. Ohta, W. Zhang, and K. Yoshimura, J. Phys. Soc. Jpn. **76**, 34702 (2007).